11th World Congress on Computational Mechanics (WCCM XI)
5th European Conference on Computational Mechanics (ECCM V)
6th European Conference on Computational Fluid Dynamics (ECFD VI)
E. Oñate, J. Oliver and A. Huerta (Eds)

ADAPTIVE CFD-ENHANCED WINDAGE MODELLING FOR AERO ENGINE TURBINE ROTOR-STATOR CAVITIES

J. M. REY VILLAZÓN[1] AND A. KÜHHORN[1]

1 Chair of Structural Mechanics and Vehicle Vibrational Technology
Siemens-Halske-Ring 14, 03046 Cottbus, Germany
reyvilla@tu-cottbus.de
kuehhorn@tu-cottbus.de

Key Words: *Flows with heat transfer, Sensitivity Analysis, Internal Air System, CAE and finite element integrations, Cavity flows, Windage, Turbomachinery, Aero Engine.*

Abstract. *The rotating components in aero engines are highly stressed as a result of the centrifugal and thermal loads. The turbine discs are embedded in the secondary air system (SAS), which is defined as the air flows that are not directly contributing to engine thrust. One of the main functions of the SAS is to ensure that the rotating components are surrounded by fluid conditions that optimize their life and integrity. This paper describes a novel approach to automatically adapt SAS heat transfer models in the turbine preliminary design phase. The proposed techniques allow fast scaling of varying disc cavity flows and heat transfer effects, to be able to cope with changes in turbine topology.*

A comparison between a theoretical calculation and the prediction of the proposed CFD-enhanced flow network model puts forward the relevance of the local flow field effects in the design concept of the SAS. As a conclusion, the paper shows how the SAS design variations can have a significant influence on the high pressure turbine (HPT) overall power and the air that is fed back into the turbine blade rows.

Nomenclature.

Abbreviation	Description	Abbreviation	Description
CFD	Computational Fluid Dynamics	RRD	Rolls-Royce Deutschland Ltd & Co KG
DOE	Design of Experiment	SAS	Secondary Air System
HP	High Pressure	SFC	Specific Fuel Consumption
HPT	High Pressure Turbine	SN	Swirl Number
HTC	Heat Transfer Coefficient	$\dot{W}_{SAS}$	Power input in SAS model
HPU	Heat Pick-up	$\dot{W}_{HP}$	Power input overall HP system

1 INTRODUCTION

The secondary air system is the part of the engine heat management system responsible for internal flows and external bleed systems. This paper deals with the internal cooling and sealing air, more specifically, with the front HPT internal flows, as they affect the overall efficiency of the turbine. Figure 1 shows a typical two-stage HPT configuration of an aero engine, on the left side, with a sketch of SAS flows around the turbine discs, on the right side.

A main function of the SAS is to provide turbine blade cooling supply and rim sealing for the turbine annulus. However, these blade cooling and rim sealing flows degrade the aerodynamic efficiency of the turbine. The SAS design process needs to take into account that the internal air is returned to the main annulus at a lower state of enthalpy than when it was bled off. This implies that a portion of the work that could have been done by the turbine is lost or transferred as heat in the internal components.

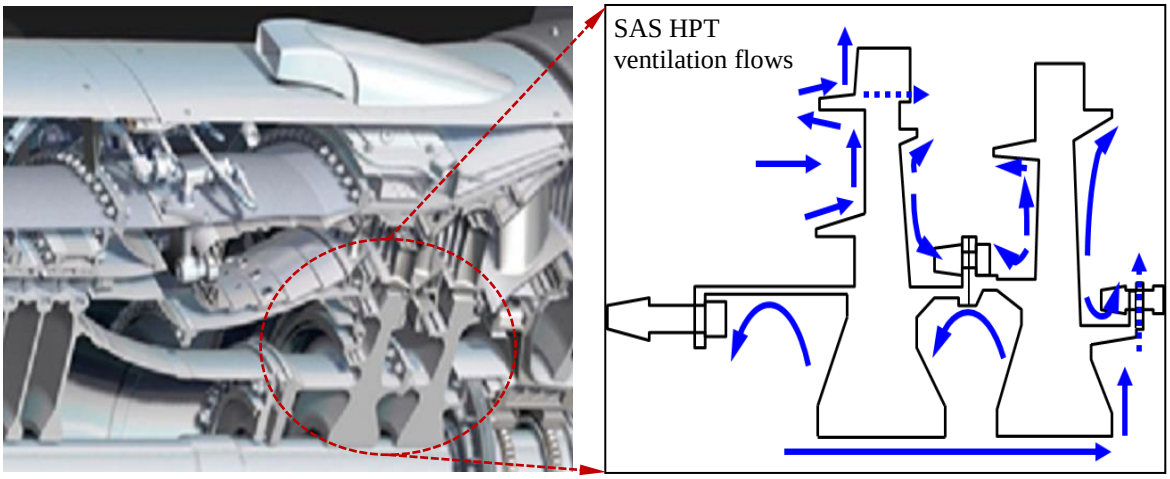

Figure 1: Aero engine 2-stage HPT cutaway (left) & SAS disc cavity ventilation flows (right). Courtesy of Rolls-Royce Deutschland

The investigations carried out in [1] put forward the relevance that the SAS flows have on disc lifing and stress targets. Hence, the SAS design also needs to optimize the ventilation flows around the disc's cavities. An important contribution to the total temperature of these flows is the phenomenon known as windage, as well as the pumping moment required to bring the fluid from the cavities to the higher radius and rotating speed of the blade cooling channels.

The secondary air system of an engine is commonly modelled by a one dimensional flow network, consisting of nodes and links. This abstraction can be viewed as a series of cavities or chambers, linked by flow passages. The approach was originally proposed in [2], who presented a method based on successive corrections for solving the problem of distribution of flows and loss of pressure head (static pressure) in networks of pipes. The fundamentals of a computer program to solve the flow network was first published by [3] and [4].

Since the pattern of the flow in the SAS is 3D or in the simplest cases 2D, the SAS model developer needs to reduce the real flow characteristics in the 1D flow network. To capture the 3D effects, experimental results or CFD solutions can be used to come up with acceptable correlations that are embedded in the 1D flow network. CFD was already considered as a high potential tool for the analysis of the SAS in [5]. At the early state of CFD simulation there was no confidence in the ability to produce validated methods. However nowadays, as stated in [6], "CFD is used with some confidence in industry and is considered essential as a research tool".

This paper presents a novel preliminary design method to calculate the power losses of the SAS flows around turbine discs. At first, a theoretical study of flow field phenomena is presented, which leads to an understanding of the relevant non-dimensional parameters. Thereafter, the proposed approach is introduced, where a parametric 1D-flow network model of the application case is enhanced with local flow field information from CFD simulations and empirical correlations. A parametric CFD process is set up to conduct design of experiments (DOEs) of the flow field thermal properties. The output from the CFD automated simulations is used to enhance the thermal functions that describe heat transfer between the fluid and solid walls.

The CFD-enhanced flow network model is used to perform a parametric study of the impact of the SAS design variables on the turbine power losses. The windage and pumping power losses of the HPT front SAS features can account for a significant percentage of the overall turbine power. According to [7], an increase of the Specific Fuel Consumption (SFC) by 1% can result in an increase of the operational costs of the engine by 0.5%. The impact of the SAS design is then critical, taking into account that in modern aero engines a 1% secondary air increase, corresponds to a SFC from 0.4% to 0.6%, as stated in [7].

2 DESCRIPTION OF APPLICATION CASE

The application case of this research focuses on the front cavities of a typical aero engine HPT. The HPT components operate at high temperatures and rotating speeds in the engine, which makes their performance highly dependent on the flow field phenomena.

Figure 2 shows a sketch of the baseline SAS configuration and Table 1 presents a summary of the SAS cavities and features that will be relevant throughout the investigation. The baseline geometry dimensions and operation parameters have been taken from a typical in-service two-stage HP turbine.

There are five boundaries to the model. The inlet flow boundaries are the air flows into cavities C and D, which come from two separate off-takes in the high pressure compressor. In cavity A, the air sinks through the rim gap into the main annulus. The mass flow and outlet conditions of the air in the blade cooling and firtree channels flowing to the next turbine stage are also considered as boundaries to the system.

Table 1: Description of the application internal air system configuration

Air system feature	Description	Operation
Cavity A	rim rotor-stator	radial outflow
Cavity B	mid rotor-stator	radial outflow
Cavity C	only static walls	axial flow
Cavity D	axial rotor-stator	axial flow
Seal A	labyrinth seal	feeds cavity B
Seal B	double labyrinth seal	feeds cavity A
Pre-swirl hole	skewed hole	feeds cavity B
Firtree	blade-disc slots	axial flow
Blade cooling	rotating channel	radial outflow

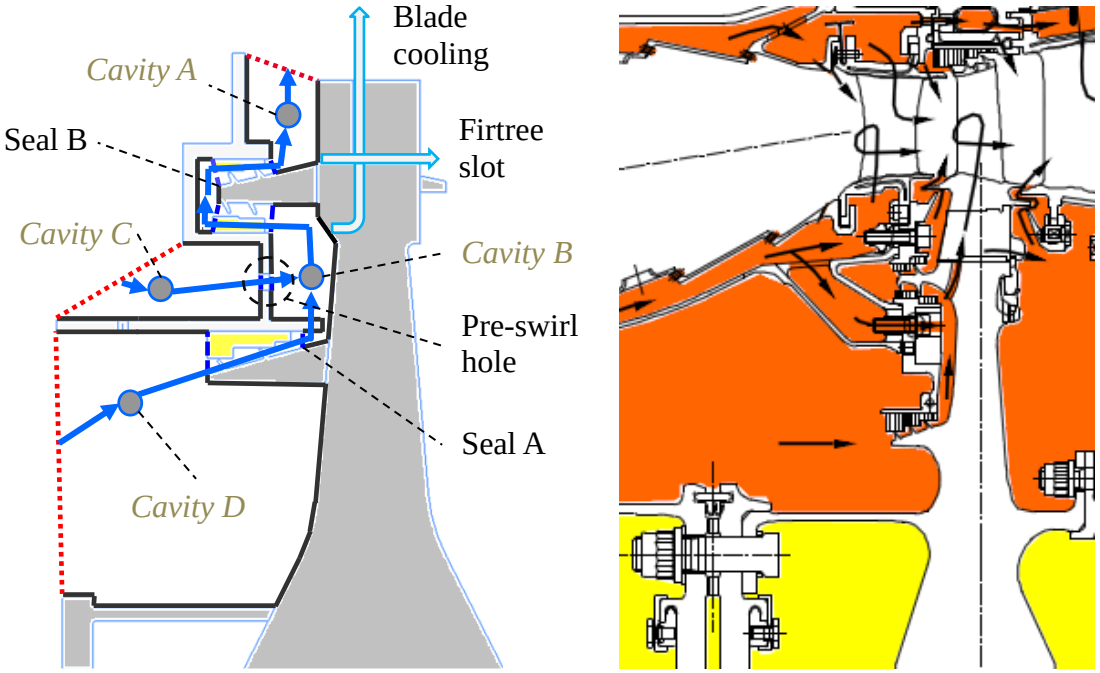

Figure 2: Configuration of the HPT front application case SAS features (left); and diagram of the SAS flows in a realistic turbine geometry (right)

3 THEORETICAL POWER LOSSES

Windage is defined as the power applied by the rotor moment on the fluid bathing it. The change in specific total enthalpy of a fluid flowing stationary through a control volume can be calculated with the first law of thermodynamics. For a perfect gas, the change in specific total enthalpy can be expressed as a function of total temperature, and it can be related to the heat

and power input as in equation (1).

$$\dot{Q} + \dot{W} = \dot{H}_2 - \dot{H}_1 = \dot{m} \cdot c_p \cdot \left(T_{t,2} - T_{t,1}\right) \tag{1}$$

The heat term is associated to convective heat transfer and sometimes even a source of radiation. If the system is considered to be adiabatic, $\dot{Q}$ will be zero. The term $\dot{W}$ is the power that is put into the fluid system by the disc. It includes what is commonly known as viscous heating or windage $\dot{W} = \Omega \cdot M$.

The term M represents the torque for one wetted side of the disc, as in the equation (2) below, where $\tau_{\varphi,w}$ is the tangential shear stress at the wall.

$$M = -2\pi \int_{r_1}^{r_2} r^2 \tau_{\phi,w}\, dr \tag{2}$$

The torque can be described with the dimensionless moment coefficient c_m for a complete disc (2 wetted sides), as in (3).

$$c_m = \frac{M}{\rho/2 \cdot \Omega^2 \cdot r_2^{\,5}} \tag{3}$$

When combining the above formulation, it can be concluded that windage changes the total temperature of the fluid from the inlet to the outlet of a control volume, as expressed in (4).

$$\Delta T_{\dot{W}} = \frac{c_m \cdot \rho/2 \cdot \Omega^3 \cdot r_2^{\,5}}{\dot{m} \cdot c_p} \tag{4}$$

The main sources of windage losses in the SAS of a turbine are the disc and cylinder surfaces, labyrinth and brush seals, and rotating protrusions such as bolts. Other phenomena that contribute to power losses are the blade cooling channel pumping and the change in fluid tangential velocity when entering rotating channels (e.g. the firtree slot).

Regarding the windage losses of rotor-stator cavities, enclosed discs without cavity through flow have a similar behavior as free rotating discs. But the c_m of the enclosed disc drops with the Re_φ due to the recirculation air. However, the cavity through flow exchanges the recirculation air by fresh inlet air. This in turn causes c_m to increase into the order of the free rotating disc, an effect that is in depth described in [8]. Thus, as an approximation, the free disc correlation from [9] will be used for radial rotor-stator cavities with through flow, equation (5).

$$c_m^{\,rad} = 0.042 \cdot \mathrm{Re}_\varphi^{-0.122} \tag{5}$$

When the fluid enters a rotating channel from a cavity where the swirl number is below 1, there is power needed to increase the tangential velocity of the flow and to pump the flow from a lower to a higher radius. These effects can be simplistically calculated by the Euler's pump and turbine equation of turbo-machinery, equation (6).

$$\dot{W} = \dot{m} \cdot \left(u_{\varphi,2} \cdot \Omega \cdot r_2 - u_{\varphi,1} \cdot \Omega \cdot r_1 \right) \tag{6}$$

For labyrinth seals, the windage power is calculated from a semi-empirical correlation of c_m^{seal}. A similar approach is followed for the windage of cylindrical rotor-stator cavities, where a semi-empirical correlation of c_m^{cyl} is integrated along the length of the cylinder. For realistic applications, experimentally based matching factors are used to adequate the c_m correlations to actual engine operation and geometry conditions. Taking the above considerations, the theoretical power losses of the SAS features are summarized in Table 2:

Table 2: Windage and pumping power equations for the HPT SAS features

Feature	Topology	Power equation
Cavity	radial rotor-stator	$\dot{W} = c_m^{rad} \cdot \rho / 2 \cdot \Omega^3 \cdot (r_2^5 - r_1^5)$
Cavity	only static walls	*Null*
Cavity	axial rotor-stator	$\dot{W} = c_m^{cyl} \cdot \rho / 2 \cdot \pi \cdot \Omega^3 \cdot r^4 \cdot L$
Seal	labyrinth seal	$\dot{W} = c_m^{seal} \cdot \rho / 2 \cdot \pi \cdot \Omega^3 \cdot r^4 \cdot L$
Blade feed inlet	swirl increase	$\dot{W} = \dot{m} \cdot \Omega^2 \cdot r^2 \cdot (1 - S_R)$
Blade cooling Δr	radial rotating channel	$\dot{W} = \dot{m} \cdot \Omega^2 \cdot (r_2^2 - r_1^2)$
Firtree	swirl increase	$\dot{W} = \dot{m} \cdot \Omega^2 \cdot r^2 \cdot (1 - S_R)$

4 CFD ENHANCED HEAT TRANSFER FUNCTIONS

Heat transfer functions are used to model the thermodynamic interaction between fluid and solid walls in the air system flow network. The approach presented in this paper consists on enhancing the heat transfer functions with 3D flow field information from CFD simulations. Four basic flow field properties carry the heat transfer information between solid and fluid domains: mass flow, swirl number (SN), heat transfer coefficient (HTC), and heat pick up (HPU) due to rotational power (i.e. windage).

In the approach presented in this paper, each of the four thermal properties is built from 3 part functions, as exemplified for the HTC in equation (7):

1. dependency to geometry profile extracted from CFD: $f^{input}(x_i)$,
2. correlation to engine operation parameters: $g^{input}(\Omega)$,
3. dependency to cavity topology via a factor from the parametric CFD, which scales the input when dimensions are varied: $Fc^{input}_{CFD}(cavity)$.

$$HTC = f^{HTC}(r) \cdot g^{HTC}(\Omega) \cdot Fc^{HTC}{}_{CFD}(cavity) \tag{7}$$

The CFD was pre-run on some typical cavities. As a result, generalized surrogate functions were extracted that can be used for the same cavity types in any new designs. These CFD-surrogate models are used as long as the cavities of the new design are analogous to the pre-run cavities. The surrogate CFD functions should be newly generated for designs with completely new cavity topology. As an example, the development of the CFD-enhanced heat transfer functions will be demonstrated for the topology: rotor-stator cavity (e.g. cavity B).

4.1 Parametric CFD process

In order to generate the heat transfer functions that have been described in the previous section, an automated CFD process has been set up. A diagram of the coupled workflow is shown in Figure 3.

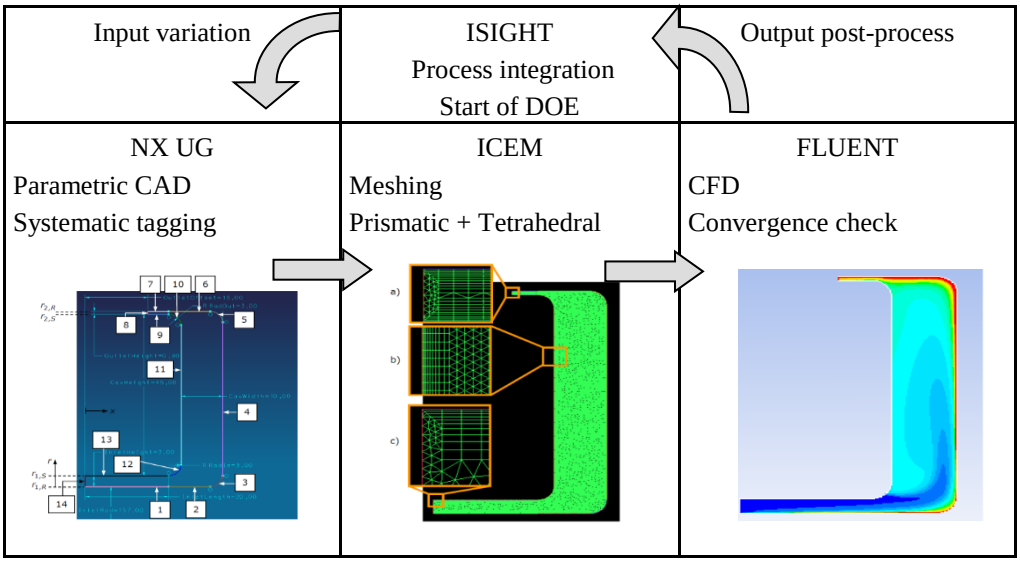

Figure 3: Parametric CFD workflow and coupled applications

The software Isight is used as a tool integrator, and as a means to generate the population of DOE studies. The geometry input in the automated workflow is a tagged sketch CAD model of the cavity fluid domain. The model is meshed automatically (in ICEM CFD), where the geometry tags allow the application of different mesh settings to different model boundaries. The meshed model is then transferred into the CFD solver (FLUENT), boundary conditions and settings are loaded via script, and the solver is run automatically.

4.2 CFD generated heat transfer functions

The functions that represent heat transfer mechanisms of cavities in the internal air system flow network are derived from the CFD models generated with the previously described workflow. The mass flow and swirl number distributions can be directly extracted from the CFD output. However, the HTC and windage HPU functions require some post-processing from CFD. The HTC is determined via Reynolds analogy, equation (8), and the windage

power input is calculated as the moment of the wall shear stresses, equation (9).

$$HTC(r) = \frac{\tau_{\varphi}(r) \cdot c_p(r)}{u_{\varphi}(r) \cdot (\mathrm{Pr})^{0.4}} \tag{8}$$

$$\dot{w} = \tau_{\varphi}(r) \cdot \Omega \cdot r \tag{9}$$

As an example of the CFD extracted heat transfer functions, Figure 4 shows the heat transfer coefficient profile along rotor radius for a typical turbine rotor-stator cavity. The plot compares the CFD extracted data with a traditional 1D flow network thermal function and the new CFD-enhanced thermal function. The piece-wise linear function that approximates the CFD data, rather than the raw CFD data itself, is what will be implemented in the SAS flow network model.

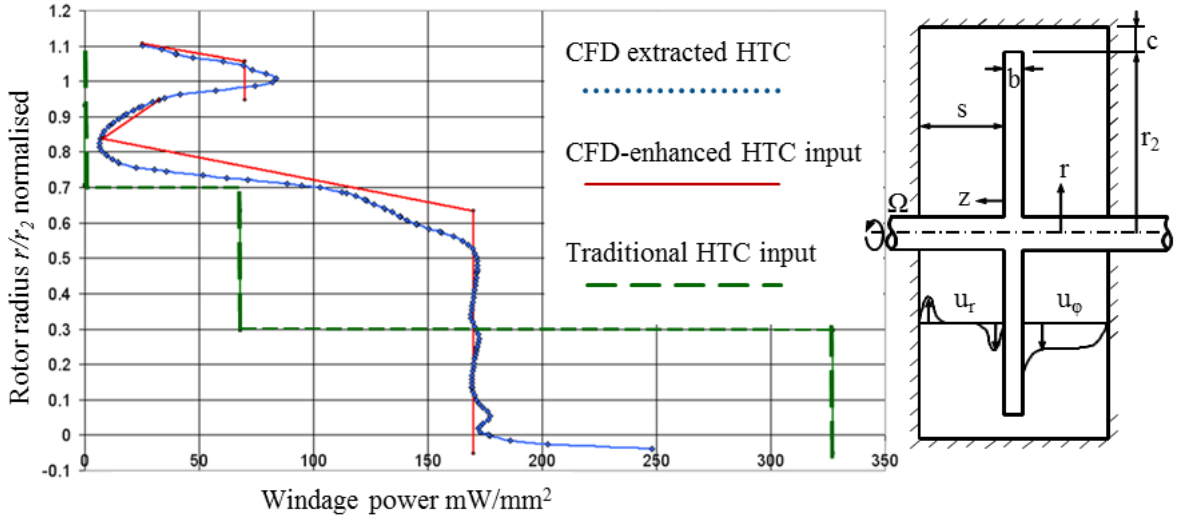

Figure 4: Radial distribution of rotor windage in a typical turbine rotor-stator cavity

The HTC radial profile from Figure 4 is then combined with the functions of operation and cavity topology dependency, as shown in (7). The function of cavity topology is generated through a DOE set of analyses with the parametric CFD process. In this investigation, a polynomial approximation as in (10) was chosen, which best fitted the CFD results across the design space of the cavity parameters (x_i normalized with its baseline value $x_{i,BL}$). The authors in [10] present a description of how the CFD-enhanced heat transfer functions have been verified against engine experimental thermal survey data.

$$F^{HTC} = C_0 + \sum_{i=1}^{n} C_i \cdot \frac{x_i}{x_{i,BL}} \tag{10}$$

5 ENHANCED FLOW NETWORK POWER LOSSES CALCULATION

The proposed approach for the SAS power loss calculation consists on a parametric 1D flow network model, enhanced with local flow field information. Figure 5, left side, shows the flow network for the HPT front application case. The 1D-cavity bits in the network that calculate power, swirl and total temperature changes due to windage are enhanced with the data extracted from the parametric CFD calculations.

The power losses of the baseline SAS configuration have been calculated using both: the theoretical functions from the introductory chapter and the CFD-enhanced 1D flow network. A comparison of the results is presented in Figure 5, right side. As an outcome, the flow network windage losses in the rotor-stator cavities are smaller than the ones from the theoretical calculation. The difference on integral HPT SAS power loss between the enhanced flow network and the theoretical model is 12%, which accounts for a tenth of the overall turbine efficiency.

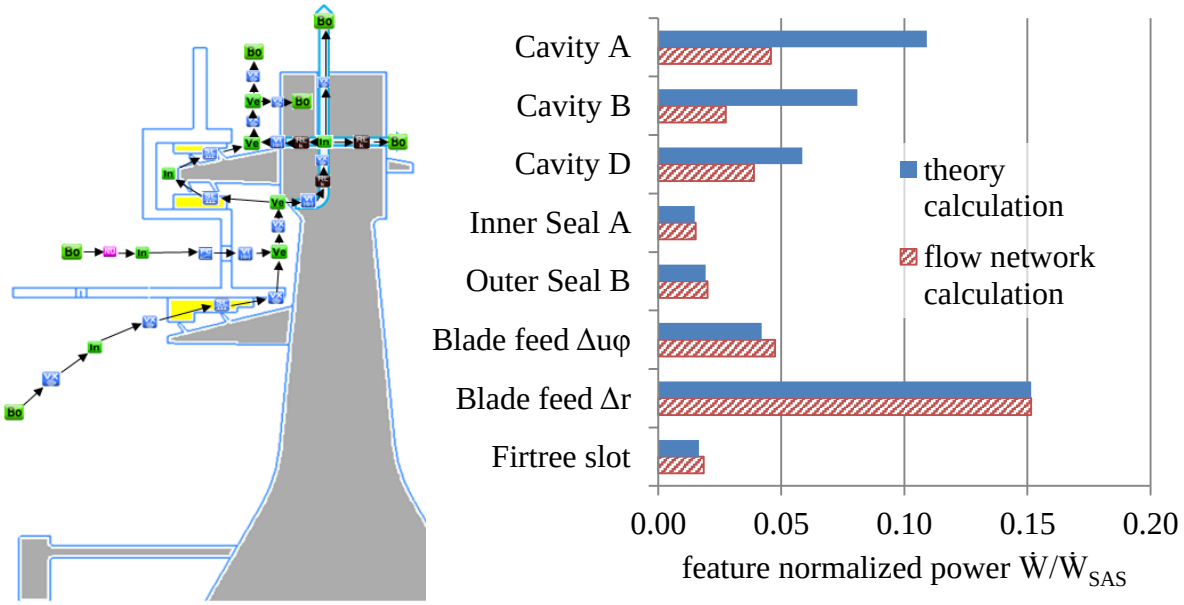

Figure 5: 1D flow network model of the HPT SAS (left); and comparison of the front HPT SAS power losses calculated with the enhanced flow network model and the theoretical approach, normalized with $\dot{W}_{SAS}$ (right)

6 DESIGN TOPOLOGY PARAMETER STUDY

Taking the previously presented front HPT SAS configuration as the baseline geometry, the following variations are applied in the parameter study:

- Scaling of the main annulus inner rim radii (constant axial gaps).
- Radial rotor-stator cavity gaps.
- Pre-swirl system radius and skew angle.
- Seal radii.
- Operation speed.

The parameter investigation in this paper focus on turbine power losses and disc ventilation flows. Nonetheless, it should be mentioned that the proposed variations would have consequences in engine bearing loads, performance, manufacturing costs, and robustness. A realistic design should take trade-offs for all of these disciplines into account.

Each design parameter has been varied from the baseline in a bandwidth of ±10%. The following results present a summary of how these variations affect the individual and combined power loss of the HPT SAS features. Figure 6 shows each parameter's impact on the overall power loss of the front HPT SAS.

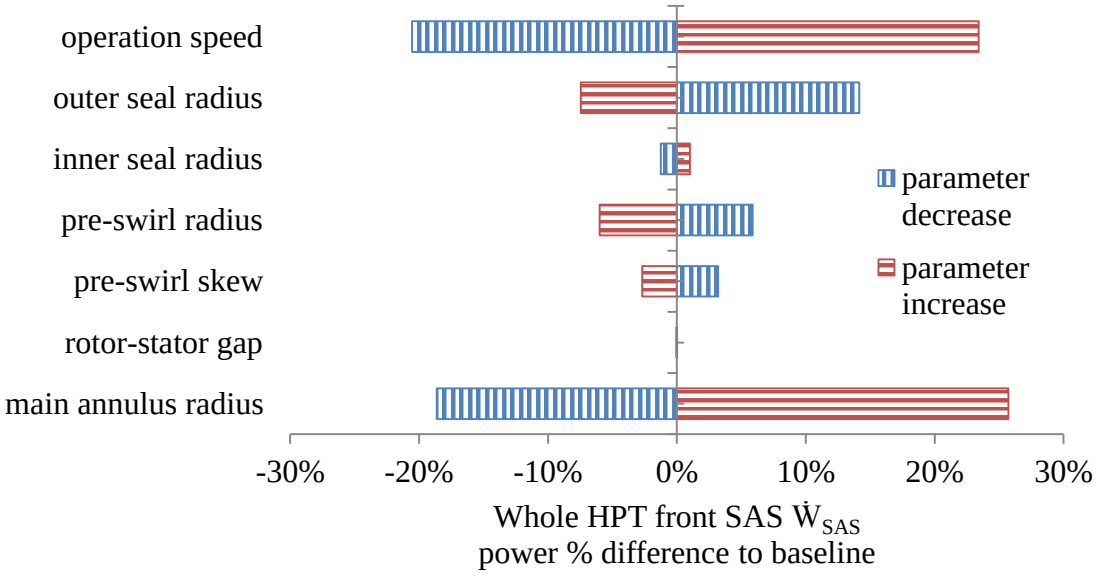

Figure 6: Percentage impact of each SAS design variation on the power loss of the whole HPT front SAS. The baseline whole SAS power loss is the addition of the individual feature powers, presented in Figure 5.

The highest impact on the power loss is the one from the main annulus radii changes, which are common during initial design stages. Rim line modifications shift the radial position of the cavities, leading to variations of the rotor wall area that directly affect the viscous heating surface. The seal radii change also implies higher surface and rotor wall tangential speed, thus higher windage. In summary of the results, the assessed SAS design changes have a considerable impact on the overall HPT power $\dot{W}_{HP}$. For example, the +10% scaling of main annulus radius results in up to 0.2% change of the total HP power. The positions of the seals and pre-swirl also have a considerable impact, which could be used on the benefit of a design optimization. From these results, conclusions are drawn in the following chapter.

7 CONCLUSIONS

- A 1D-flow network model of the HPT front SAS has been enhanced with local flow field data from pre-run CFD simulations. The enhanced network model offers a quick solution, while providing a good level of fidelity for the preliminary design phase.

- The CFD-enhanced heat transfer functions are built from three parts: the 1st part carries detail CFD flow field distribution information; the 2nd part includes the correlation to turbine operation parameters, and the 3rd one contains the information of dependency to cavity topology and dimensions that has been gathered from a DOE of parametric CFD simulations.

- The difference on estimated HPT front power loss between the theoretical and enhanced flow network calculations is 12%. These power losses add up to 0.83% of the overall high pressure turbine power, which is a relevant order of magnitude for a competitive SFC in the aero engine industry.

- The 1D-flow network model enables design variation studies to assess the impact and interdependencies of the SAS parameters on windage and pumping power losses. To this effect, the new CFD-enhanced flow network adapts the flow field calculations and heat transfer functions to changes in the cavity topology.

- A sensitivity study on SAS design variations shows that rim line radius scaling and operation speed are the most relevant parameters that affect the HPT SAS power losses. The biggest contributor to the power losses is the pumping power required to feed the blade cooling system. Moreover, the effect of windage in rotor-stator cavities should not be underestimated in designs with very large radial cavities, since it has a strong dependency to radius variations: r_2^5-r_1^5.

- This investigation focused on variations of the front HPT SAS design, which lead to deviations on HP overall power by tenths of a percent. When considering the complete SAS, there is a relevant HP power optimization potential for the gas turbine community.

8 ACKNOWLEDGEMENT

This work has been carried out in collaboration with Rolls-Royce Deutschland as part of the research project VIT 3 (Virtual Turbomachinery, contract no. 80142272) funded by the State of Brandenburg and Rolls-Royce Deutschland. Rolls-Royce Deutschland's permission to publish this work is greatly acknowledged.

Very valuable support has been provided by the fluids systems and the turbines aero-thermal department at Rolls-Royce Deutschland.

REFERENCES

[1] Rey Villazon, J. M, T. Weiss, and Kühhorn A, "A Parametric Impact Study Of The Geometry, Air System And Thermal Boundary Conditions On The Life Of A Two-Stage High Pressure Turbine," in *Proceedings of the ASME Turbo Expo 2012: Turbine Technical Conference and Exposition*, New York, N.Y: The American Society of Mechanical Engineers, 2012.

[2] H. Cross, *Analysis of flow in networks of conduits or conductors*. Urbana, Ill: University of Illinois, 1936.

[3] K. J. Kutz and T. M. Speer, "Simulation of the Secondary Air System of Aero Engines," *J. Turbomach*, vol. 116, no. 2, p. 306, 1994.

[4] A. Majumdar, *A generalized fluid system simulation program to model flow distribution in fluid networks*. Washington, DC, Springfield, Va: National Aeronautics and Space Administration; National Technical Information Service, distributor, 1998.

[5] H. Zimmermann, "Some Aerodynamic Aspects of Engine Secondary Air Systems," *J. Eng. Gas Turbines Power*, vol. 112, no. 2, p. 223, 1990.

[6] J. W. Chew and N. J. Hills, "Computational fluid dynamics for turbomachinery internal air systems," (eng), *Philos Trans A Math Phys Eng Sci*, vol. 365, no. 1859, pp. 2587–2611, 2007.

[7] A. B. Turner, C. A. Long, Childs, P.R.N, N. J. Hills, and J. A. Millward, "A review of some current problems in gas turbine internal air systems," in *ASME Aeroengine Congress*, 1997.

[8] J. W. Daily and R. E. Nece, *Roughness and chamber dimension effects on induced flow and frictional resistance of enclosed rotating disks*. [Cambridge, Mass.]: Hydrodynamics Laboratory, Dept. of Civil and Sanitary Engineering, Massachusetts Institute of Technology, 1958.

[9] L. A. Dorfman, *Hydrodynamic resistance and the heat loss of rotating solids*, 1st ed. Edinburgh: Oliver & Boyd, 1963.

[10] Rey Villazon, J. M, M. Berthold, and Kühhorn A, "Adaptive Flow Field Thermal Modeling Techniques for Turbine Rotor-Stator Cavities," in *Proceedings of the ASME Turbo Expo 2013: Turbine Technical Conference and Exposition*, 2013.